INTERNATIONAL JOURNAL FOR NUMERICAL METHODS IN ENGINEERING
Int. J. Numer. Meth. Engng 2015; **102**:1750–1760
Published online 28 January 2015 in Wiley Online Library (wileyonlinelibrary.com). DOI: 10.1002/nme.4869

A stabilized central difference scheme for dynamic analysis

Georg Großeholz[1,*,†], Delfim Soares Jr.[2] and Otto von Estorff[1]

[1]*Institute of Modelling and Computation, Hamburg University of Technology, Hamburg 21073, Germany*
[2]*Structural Engineering Department, Federal University of Juiz de Fora, Juiz de Fora, MG, Brazil*

SUMMARY

In this work, a new, unconditionally stable, time marching procedure for dynamic analyses is presented. The scheme is derived from the standard central difference approximation, with stabilization being provided by a consistent perturbation of the original problem. Because the method only involves constitutive variables that are already available from computations at previous time steps, iterative procedures are not required to establish equilibrium when nonlinear models are focused, allowing more efficient analyses to be obtained. The theoretical properties of the proposed scheme are discussed taking into account standard stability and accuracy analyses, indicating the excellent performance of the new technique. At the end of the contribution, representative nonlinear numerical examples are studied, further illustrating the effectiveness of the new technique. Numerical results obtained by the standard central difference procedure and the implicit constant average acceleration method are also presented along the text for comparison. Copyright © 2015 John Wiley & Sons, Ltd.

Received 5 August 2014; Revised 11 December 2014; Accepted 12 December 2014

KEY WORDS: time marching; dynamic analysis; unconditional stability; nonlinear iteration; central differences; constant average acceleration method

1. INTRODUCTION

Direct time integration is a commonly used technique in numerical simulation of dynamic systems, occurring in various branches of science and practical engineering design. The rigorous investigation of these schemes has a long tradition in the field of applied mathematics and numerous books and articles addressing this issue have been published in the last decades [1–19]. In general, direct time marching procedures can be subdivided into two families, namely explicit methods and implicit methods. In an explicit approach all constitutive variables are available from computations at previous time-steps and, in combination with diagonal matrices, these methods do not require the solution of any system of equations. In an implicit approach, on the other hand, the constitutive variables are expressed as functions of the current time of analysis. In this case, when nonlinear models are focused, the solution has to be carried out by iterative schemes, such as the Newton–Raphson algorithm, which always cause a significant overhead in the computational effort. Moreover, these iterative procedures may cause numerical issues affiliated to the convergence behavior. As a consequence, the computational cost of an implicit analysis may significantly exceed that of an explicit solution.

On the other hand, standard explicit approaches have restrictive limitations for the incremental time step size Δt because of conditional stability. These restrictions usually impose an increase in the computational cost of the analysis, because a higher number of time steps is then necessary

*Correspondence to: Georg Großeholz, Institute of Modelling and Computation, Hamburg University of Technology, 21073 Hamburg, Germany.
†E-mail: grosseholz@tuhh.de

to provide a solution. Moreover, this critical time step can be quite hard to estimate (if it is not impossible), when complex nonlinear models are considered.

In order to combine the advantages of both explicit and implicit families, hybrid methods have been developed. Some of them are referred to as 'linearly implicit' [5–7], others are referred to as 'nonlinearly explicit' [8–12]. These schemes are comparable with an implicit approach, in the linear case, while, in the nonlinear case, no iterative procedures are needed. The so-called Rosenbrock–Wanner methods, described in [5–7], are based on sophisticated implicit Runge–Kutta methods [3]. The schemes presented in [8, 9] are more simple and spectrally equivalent to the constant average acceleration method (CAAM), also known as trapezoidal rule. The second order accurate, explicit approaches presented in [10–12] and in [13] are strongly related to the standard central difference procedure, but they introduce numerical damping into the computed results, rendering a dissipative scheme. The present method is a stabilized, non-dissipative central difference (CD) scheme and the restrictive step size limitation of the standard CD approximation is circumvented by a consistent perturbation of the analyzed system. This perturbation approach may be interpreted as a selective mass scaling, as presented in [20, 21] and further developed in [22–26]; however, these publications focus on aspects of spatial discretization, consequently no theoretical accuracy and stability analysis is provided, as it is the case in the present work (Section 3). Here, the standard mass matrix is consistently combined with the tangent stiffness matrix, rendering a modified non-diagonal mass matrix. Thus, a linear system of equations has to be dealt with at each time step of the analysis. However, because all constitutive variables are available from computations at previous time-steps, no iterative procedure is needed when nonlinear models are considered. As a consequence, the method provides accurate and stable results at reasonable computational costs. In the next section, the standard CD procedure is briefly summarized, and the stabilized CD is introduced. In Section 3, stability and accuracy analyses are carried out. Finally, in Section 4, three numerical examples are presented, illustrating the performance and potentialities of the proposed technique.

2. TIME DISCRETIZATION

The solution of the undamped equation of motion

$$\ddot{u} + F(u) = r \tag{1a}$$

$$u(t=0) = f, \quad \dot{u}(t=0) = g \tag{1b}$$

accompanied by initial conditions $f, g \in \mathbb{R}^n$ is essential in many engineering applications. Here and in the following, $u \in \mathbb{R}^n$ represents the exact displacements of the $n \geqslant 1$ DOF of the considered system, while one and two over dots denote its first and second derivative with respect to time, respectively. The $r \in \mathbb{R}^n$ stands for the relation of the applied force terms and the mass of the system, while $F : \mathbb{R}^n \to \mathbb{R}^n$ accounts for the relation of the stiffness and the mass of the system in dependence of the displacements.

The well-established acceleration-based form of the CD formulation

$$U_{n+1} = U_n + \Delta t \dot{U}_n + 0.5\Delta t^2 \ddot{U}_n \tag{2a}$$

$$\dot{U}_{n+1} = \dot{U}_n + 0.5\Delta t(\ddot{U}_n + \ddot{U}_{n+1}) \tag{2b}$$

is spectrally equivalent to the standard three-point-star approximation

$$\ddot{U}_n = \frac{1}{\Delta t^2}(U_{n+1} - 2U_n + U_{n-1}) \tag{3a}$$

$$\dot{U}_n = \frac{1}{2\Delta t}(U_{n+1} - U_{n-1}). \tag{3b}$$

DOI: 10.1002/nme

In this context, Δt denotes the incremental time step, while $U_n, \dot{U}_n$, and $\ddot{U}_n$ represent the approximate solutions to the exact displacements, velocities, and accelerations at time $t = n\Delta t$, respectively. Because $U_0 = f$ and $\dot{U}_0 = g$ are given as initial conditions, only $\ddot{U}_0$ needs to be computed by establishing equilibrium in Equation (1a) at time $t = 0$. Afterwards, U_1 can be computed according to Equation (2a) without any reformulation; therefore, the acceleration-based form is called self-starting. Again, displacements, as well as velocities and accelerations, need to be computed at each time step during the time marching process, even if only the displacements are sought for. The three-point-star approximation, on the other hand, only involves displacement values and it is not self-starting. Once U_n and U_{n-1} are needed in order to calculate U_{n+1}, an alternative, self-starting formulation, like the acceleration-based form, has to be applied for the first time step. In the central difference method, the stability limit for the time increment is found to be

$$\Delta t_{crit}\omega \leqslant 2, \tag{4}$$

where ω denotes the highest natural frequency of the considered problem. The favorable features of the CD method – like its high efficiency and accuracy – are often counterpartyed by the step size limitation given in Equation (4). If the considered problem exhibits at least one very large natural frequency, which might even have a negligibly small contribution to the solution, the critical time increment Δt_{crit} becomes very small. Consequently, the solution may become quite computationally demanding or even impractical, because a huge amount of time steps may be needed to be employed. This becomes especially critical if non-diagonal mass matrices are considered, and solver procedures are required at each time step.

2.1. Stabilized central differences

In order to stabilize the standard CD procedure, the original problem (1) is first perturbed, leading to

$$(I + a\Delta t^2 DF|_u)\ddot{u} + F(u) = r \tag{5}$$

and discretized by a CD operator afterwards. Here, I denotes the $n \times n$-dimensional identity matrix. The term $DF|_u$ denotes the Jacobian matrix of F, evaluated at u, and will be referred to as tangent matrix; $a = 0.25\tanh(\alpha\Delta t\omega)$ is a positive scalar function serving as a limiter. A proper choice for the positive constant α will be discussed during the stability analysis, in Section 3.1. The term

$$AM = a\Delta t^2 DF|_u \tag{6}$$

is an artificial mass matrix, added to the system in order to make it react slower. This approach may be interpreted as a special case of the so-called selective mass scaling, which was originally provided in [20, 21] and further developed in [22–26]. However, these publications do not focus on unconditional stability and time marching, which it is the case in the present work (Section 3.1). Here, AM is proportional to the square of the time increment, preserving convergence to the exact solution of the original problem. Therefore, the resulting method is consistent and the application of a second order accurate method to the altered problem in Equation (5) will still provide second order accuracy toward the exact solution of the original model.

For a linear operator, the stabilized CD can be regarded as a hybrid formulation of the standard CD and of the CAAM. The scalar function a ($0 \leqslant a \leqslant 0.25$) serves as a limiter, tuning between these two methods. If a equals zero, the proposed scheme becomes equivalent to the standard CD; if a equals 0.25, the proposed scheme becomes equivalent to the CAAM. For values of $\Delta t\omega$ larger than two, the standard CD becomes unstable. In the stabilized CD, otherwise, once $\Delta t\omega$ grows, a grows as well, approaching 0.25 and stabilizing the time marching procedure. For small values of $\Delta t\omega$, the standard CD technique is stable and accurate. In this case, a approaches zero, virtually annihilating the artificial mass AM. Consequently, in order to keep the stabilized CD as conformable as possible to the standard CD, it is desired to keep α minimal, without losing stability for $\Delta t\omega > 2$. For a multi DOF system, the overhead for computing the largest natural frequency exactly, as it is required by the a expression, would go far beyond the scope of reasonable computational effort. Hence, a fast and reliable estimate for ω has to be provided. In the present context, as it is indicated

DOI: 10.1002/nme

by the a expression, an overestimation for ω will not harm the stability of the method. Consequently, just an upper bound of the highest natural frequency is needed. Therefore, the spectral radius of the tangent matrix $DF|_u$ can be used, which may be estimated by means of Gerschgorin circles [27], for instance, providing a very fast computation for ω. In non-linear analyses, the value for ω can be either updated at each time step by estimating the largest eigenvalue of the updated tangent matrix, or an upper bound for ω can be determined a priori, keeping the same value for a during the whole time marching process.

3. MATHEMATICAL ANALYSES

The stability and accuracy properties of the proposed scheme are investigated by classic one DOF linear analyses. The theoretical background of this systematic approach is explicitly explained in [14, 15, 19], as well as by many other authors, and will not be repeated here. In the following, the three-point-star approximation described in Equations (3) is considered. Other central difference based methods, like the self-starting acceleration-based form (Equations (2)), the self-starting velocity-based form [16], and the so-called forward incremental displacement central difference [17] are spectrally equivalent to the three-point-star approximation. Consequently, analogous behavior is expected, and the following investigation is representative.

3.1. Stability analysis

In order to analyze the theoretical properties of the proposed scheme, the homogeneous one DOF linear model problem

$$\ddot{u} + \omega^2 u = 0 \tag{7}$$

is considered. First, Equation (7) is perturbed according to Equation (5)

$$(1 + a(\Delta t\omega)^2)\ddot{u} + \omega^2 u = 0 \tag{8}$$

afterwards the time derivative is replaced by the discrete three point star operator (Equations (3)). This results in the explicit two steps scheme

$$U_{t+\Delta t} = \left(2 - \frac{(\Delta t\omega)^2}{1 + a(\Delta t\omega)^2}\right) U_t - U_{t-\Delta t}, \tag{9}$$

which can be easily transformed to a recursive matrix form as follows:

$$\begin{bmatrix} U_{t+\Delta t} \\ U_t \end{bmatrix} = \begin{bmatrix} \left(2 - \frac{(\Delta t\omega)^2}{1+a(\Delta t\omega)^2}\right) & -1 \\ 1 & 0 \end{bmatrix} \cdot \begin{bmatrix} U_t \\ U_{t-\Delta t} \end{bmatrix} \quad \Longleftrightarrow \quad X_{n+1} = A \cdot X_n. \tag{10}$$

The stability properties of the scheme unveil after examination of the eigenvalues of the amplification matrix A. The characteristic polynomial $p(\lambda)$ reads

$$p(\lambda) = \lambda^2 - 2k\lambda + 1 \tag{11}$$

where

$$k = \left(1 - \frac{0.5(\Delta t\omega)^2}{1 + a(\Delta t\omega)^2}\right), \tag{12}$$

and its roots can be computed by

$$\lambda_{1/2} = k \pm \sqrt{k^2 - 1}. \tag{13}$$

DOI: 10.1002/nme

If $k^2 \in [0, 1]$, Equation (13) can be rearranged to become

$$\lambda_{1/2} = k \pm i\sqrt{1-k^2} = \rho \pm i\nu, \tag{14}$$

where $\rho, \nu \in \mathbb{R}$. Hence, the modulus of the eigenvalues can be computed according to the Pythagorean theorem, such that

$$|\lambda_{1/2}| = \rho^2 + \nu^2 = k^2 + 1 - k^2 = 1. \tag{15}$$

The constant α has to be determined according to the condition $k^2 \in [0, 1]$, rendering an unconditionally stable scheme. Because $k \leqslant 1$, only the relation

$$-1 \leqslant k \iff 0 \leqslant 1 + (a - 0.25)(\Delta t\omega)^2 \tag{16}$$

needs to be considered. The minimum value of α, satisfying Equation (16), can be determined by simple curve sketching. It is approximately $\alpha \approx 0.246$. In the following accuracy analysis, as well as in the numerical experiments presented in Section 4, $\alpha = 0.25$ is considered.

3.2. Accuracy analysis

The accuracy of the proposed scheme is investigated considering the relative period error P and the algorithmic damping ratio $\bar{\xi}$. P and $\bar{\xi}$ can be computed in terms of the eigenvalues $\lambda_{1/2} = \rho \pm i\nu$ as follows [15]:

$$P = \frac{\Delta t\omega}{\arctan(\nu/\rho)} - 1 \tag{17}$$

$$\bar{\xi} = -\frac{\ln(\nu^2 + \rho^2)}{2\arctan(\nu/\rho)}. \tag{18}$$

Consequently, the proposed scheme has no algorithmic damping – like the CAAM and the standard CD – resulting in a non-dissipative scheme. For comparison, the relative period errors for the stabilized CD, the standard CD, and the CAAM are plotted against $\Delta t/T$ in Figure 1. Here, $T = 2\pi/\omega$ denotes the period corresponding to the frequency ω. As one can observe, the proposed scheme exhibits the least deviation from the exact period T, describing a considerable more accurate time marching technique.

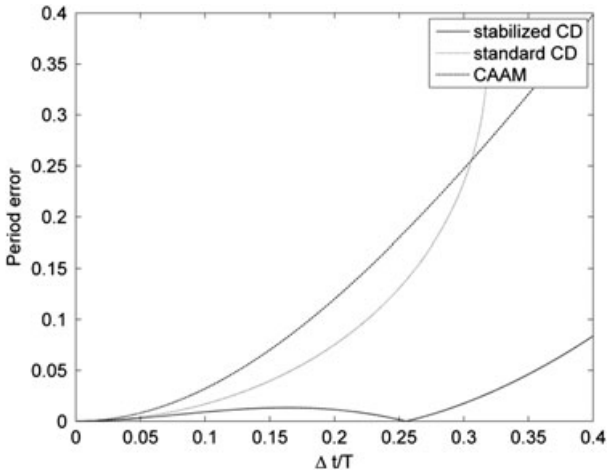

Figure 1. Period elongation modulus versus dt/T. CD, central difference; CAAM, constant average acceleration method.

DOI: 10.1002/nme

4. NUMERICAL EXAMPLES

In this section, the proposed method is tested considering three representative models. First, a linear system of ordinary differential equations (ODEs) is analyzed, followed by a nonlinear ODE of one degree of freedom. Finally, a system of nonlinear ODE, resulting from spatial semi-discretization of a nonlinear partial differential equation (PDE), is considered. Finite element (FE), as well as finite difference (FD) discretizations are applied. The proposed method is compared with the CAAM and the standard CD method. In the nonlinear cases, the CAAM has to be carried out in combination with an iterative procedure in order to establish equilibrium at each time step. Here, the commonly used Newton–Raphson method is applied. The iterative procedure is concluded when the abort criterion

$$\frac{\left\| U_{n+1}^{i} - U_{n+1}^{i-1} \right\|_2}{\max\left(\left\| U_{n+1}^{i} \right\|_2, \left\| U_{n+1}^{i-1} \right\|_2 \right)} \leqslant tol \tag{19}$$

is satisfied, where tol is a predefined tolerance and U_{n+1}^{i} and U_{n+1}^{i-1} stand for the last two iterated values of the approximate solution U_{n+1}. For the standard and the stabilized CD, no iterative procedures are necessary when nonlinear models are focused, because all constitutive variables are available from computations at previous time steps.

4.1. Linear mass-spring model

Next, an undamped three DOF system is analyzed, as described by Equations (20) as follows:

$$\begin{bmatrix} 10 & 0 & 0 \\ 0 & 10^{-6} & 0 \\ 0 & 0 & 2 \end{bmatrix} \cdot \ddot{u} + \begin{bmatrix} 1 & -1 & 0 \\ -1 & 6 & -5 \\ 0 & -5 & 5 \end{bmatrix} \cdot u = \begin{bmatrix} 1 - \sin(2t) \\ 0 \\ 0.1 \cdot (\sin(2t) - 1) \end{bmatrix}; \qquad u(0) = \dot{u}(0) = (0,0,0)^T. \tag{20}$$

A sketch of the model is depicted in Figure 2. This system exhibits a very large value for its highest natural frequency, resulting in a very small critical time increment. Consequently, a huge number of time steps has to be employed if a conditionally stable time marching procedure, like the standard CD ($\Delta t_{crit} = 0008164965$), is applied. This model can be considered a simplified representation of a large coupled system with lumped masses, where the densities of the different media differ significantly from each other. The computations are carried out taking into account five different discretization levels, and the results are compared with a reference solution, which is obtained by the standard CD with discretization of $\Delta t = 4 \cdot 10^{-5}$. In order to illustrate the convergence behavior of the three tested methods in the linear case, the relative errors of the computed results are depicted in Figure 3, along with the corresponding discretization level. In this linear example, the computational efforts for the CAAM and for the stabilized CD are comparable, because no iterations are needed. The accuracy of the stabilized CD approach, on the other hand, is better than that of the CAAM, as expected following Figure 1. As depicted in Figure 3, the standard CD is also very accurate for time steps smaller than the critical time increment. For larger time steps, however, the simulations fail because of instability.

4.2. One degree of freedom nonlinear model

In this subsection, a one DOF ODE is analyzed with a nonlinearity of polynomial form:

$$\ddot{u} + u^3 - 2u^2 - 411u + 6 = 0; \;\; u(0) = \dot{u}(0) = 0; \;\; t \in [0, 3.5]. \tag{21}$$

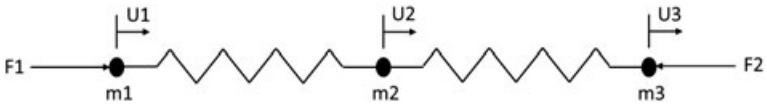

Figure 2. Sketch of the mass-spring model.

DOI: 10.1002/nme

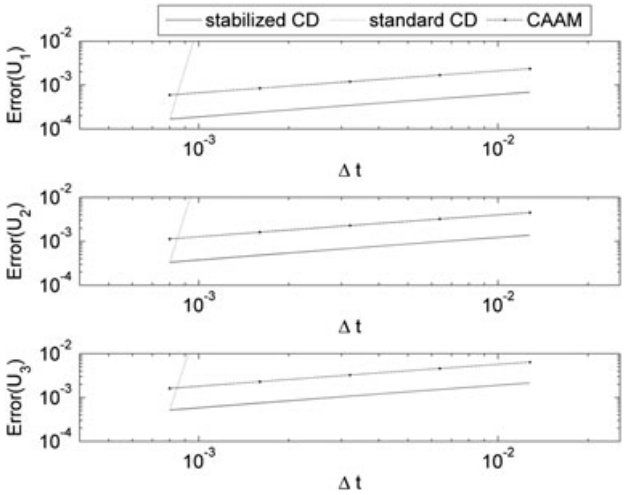

Figure 3. Relative error versus discretization for the mass-spring model. CD, central difference; CAAM, constant average acceleration method.

The example illustrates the possible sensitivity of the Newton–Raphson iterative procedure concerning the abort criterion defined by Equation (19). Although this model seems to be quite simple, its accurate simulation is very demanding and numerous adaptive ODE solvers (as implemented in many popular commercial software packages) fail when being applied to it. Because a one DOF model is considered here, the tangent matrix DF is obtained by simply deriving the nonlinear part of Equation (21) with respect to the displacement $u \in \mathbb{R}$:

$$DF = 3u^2 - 4u - 411 \tag{22}$$

The term DF is unbounded in u and consequently the highest natural frequency cannot be estimated a priori, without knowing the co-domain for the displacements. This is a crucial problem if the critical time increment for a conditionally stable method (like the standard CD) has to be determined. However, applying the stabilized CD, an a priori estimate can be made by assuming ω approaching infinity, resulting in $a = 0.25$. This overestimation for ω preserves stability at the expense of a possibly redundantly large period error. On the other hand, the value for a can be updated as the nonlinear analysis evolves. This approach bears the risk of underestimating ω for large time increments Δt and leads to additional computational effort. The following experiments are carried out with two different time increments ($\Delta t = 0.01$ and $\Delta t = 0.02$) and with four different error tolerances as abort criteria for the iterative process. The reference result is computed with the standard central difference method and $\Delta t_{ref} = 0.0001$. The time histories of the approximate displacements, along with the reference solution, are depicted in Figure 4 ($\Delta t = 0.01$) and Figure 5 ($\Delta t = 0.02$) considering four different abort criteria associated to the CAAM. For $\Delta t = 0.01$, the value ω is updated at each time step according to $\omega_i^2 = DF|_{U_i}$. The total numbers of Newton–Raphson iterations, necessary in order to establish equilibrium in combination with the CAAM, are 697 for a tolerance of 1%, 699 for a tolerance of 0.2%, 733 for a tolerance of 0.04%, and 790 when the tolerance is set to 0.008%. By comparison of the time histories for $tol = 0.2\%$ and $tol = 0.04\%$ in Figure 4, it becomes clear that the quality of the computed results does not always improve, when tol is decreased, although the computational effort does increase. On the other hand, as one can observe in Figure 4, the proposed technique provides good results without considering any associated iterative procedure, being very efficient. For $\Delta t = 0.02$, the largest natural frequency is assumed to approach infinity, and $a = 0.25$ is adopted during the whole integration. The total amounts of Newton–Raphson iterations necessary in order to establish equilibrium in combination with the CAAM are, in this case, 353 for a tolerance of 1%, 386 for a tolerance of 0.2%, 411 for a tolerance of 0.04%, and 434 when the tolerance is set to 0.008%. Because the co-domain for the displacements can now be read from Figure 4, the

DOI: 10.1002/nme

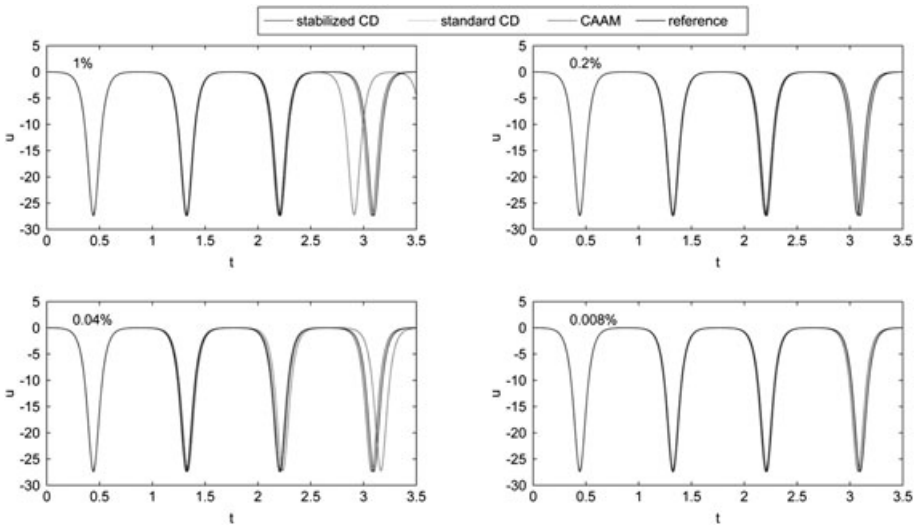

Figure 4. Time histories for the one DOF nonlinear model, considering different abort criteria for the CAAM ($\mathbf{\Delta t = 001}$). CD, central difference; CAAM, constant average acceleration method.

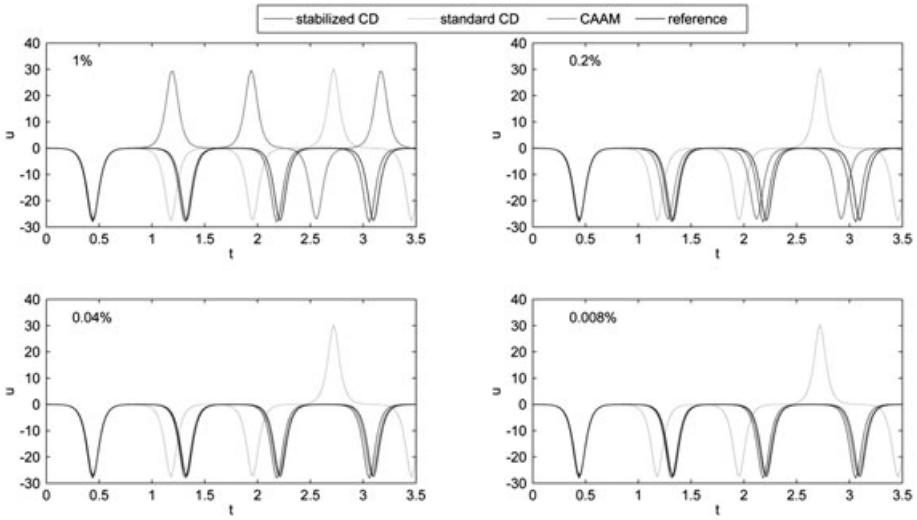

Figure 5. Time histories for the one DOF nonlinear model, considering different abort criteria for the CAAM ($\mathbf{\Delta t = 002}$). CD, central difference; CAAM, constant average acceleration method.

critical time increment is found to be $\Delta t_{crit} \approx 0.0441$. Although the critical time increment is still not exceeded here, the results obtained by the standard CD procedure are not sufficiently accurate, as shown in Figure 5. Again, the stabilized CD provides accurate results at reasonable computational cost. It is worth noting that the results obtained by the CAAM improve by decreasing tol in this case. Thus, even decreasing the time step does not necessarily lead to better results if the CAAM is applied in combination with an improper abort criterion, as it can be observed by comparison of Figures 4 and 5, for $tol = 0.04\%$.

4.3. Nonlinear partial differential equation

The third model consists of a nonlinear partial differential equation:

$$\ddot{u} - u_{xx} + \sin(u) = 0, \quad x \in \Omega; \quad \left.\frac{\partial u}{\partial n}\right|_{\Gamma} = 0. \tag{23}$$

DOI: 10.1002/nme

$$
\begin{aligned}
u(x,0) &= 4 \cdot \operatorname{atan}\left(\exp\left(\frac{x}{\sqrt{1-c^2}}\right)\right) \\
\dot{u}(x,0) &= -\frac{2c}{\sqrt{1-c^2}} \operatorname{sech}\left(\frac{x}{\sqrt{1-c^2}}\right) \\
c &= 0.2; \Omega = (-20,20); t \in [0,180]
\end{aligned} \tag{24}
$$

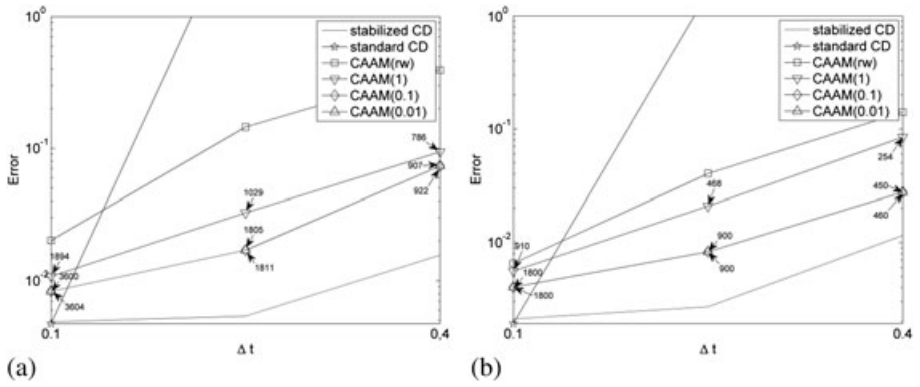

Figure 6. Relative error versus discretization for the nonlinear PDE, considering different initial conditions: (a) Equation (24) and (b) Equation (25). Spatial discretization by the finite difference method. CD, central difference; CAAM, constant average acceleration method.

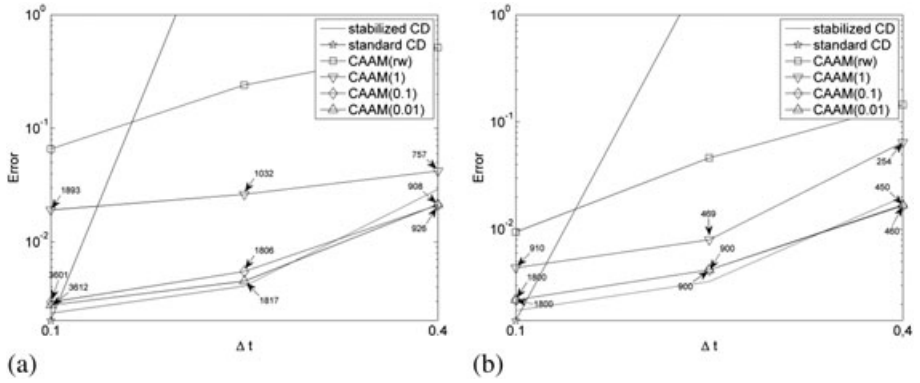

Figure 7. Relative error versus discretization for the nonlinear PDE, considering different initial conditions: (a) Equation (24); (b) Equation (25). Spatial discretization by the finite element method with lumped mass matrix. CD, central difference; CAAM, constant average acceleration method.

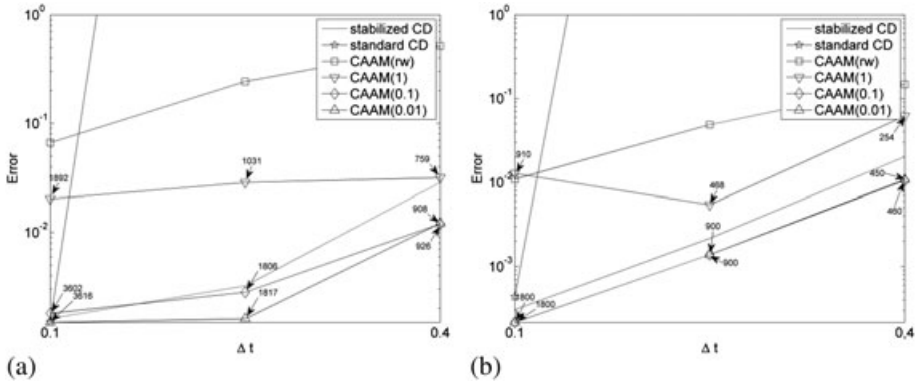

Figure 8. Relative error versus discretization for the nonlinear PDE, considering different initial conditions: (a) Equation (24) and (b) Equation (25). Spatial discretization by the finite element method with consistent mass matrix. CD, central difference; CAAM, constant average acceleration method.

DOI: 10.1002/nme

$$
\begin{gathered}
u(x,0) = 4 \cdot \operatorname{atan}\left(\exp\left(\frac{x+10}{\sqrt{1-c^2}}\right)\right) + 4 \cdot \operatorname{atan}\left(\exp\left(-\frac{x-10}{\sqrt{1-c^2}}\right)\right) \\
\dot{u}(x,0) = -\frac{4c}{\sqrt{1-c^2}} \operatorname{sech}\left(\frac{x+10}{\sqrt{1-c^2}}\right) \\
c = 0.2; \Omega = (-30, 30); t \in [0, 90]
\end{gathered} \tag{25}
$$

Here, u_{xx} represents the second derivative of the displacement with respect to the one-dimensional space. The computations are carried out considering two different sets of initial conditions (as described by Equations (24) and (25)) as well as spatial discretizations by the finite difference method (FDM) and the finite element method (FEM). When the FEM is applied, lumped and consistent mass matrixes are considered. The CAAM is tested in combination with three different abort criteria, namely $tol = 1\%, tol = 0.1\%$, and $tol = 0.01\%$. Furthermore, a direct CAAM(rw) is applied, where only one Newton–Raphson iterative step per time step is considered. The affix 'rw' is a reference to the linearly implicit Rosenbrock–Wanner methods [5–7], which are motivated by the same idea. The computational cost of the CAAM(rw) is comparable with that of the proposed stabilized method, because a linear system has to be solved only once at each time step. All experiments are performed considering three different discretization levels, namely: (a) $\Delta x = 0.2$ and $\Delta t = 0.1$; (b) $\Delta x = 0.2$ and $\Delta t = 0.2$; and (c) $\Delta x = 0.2$ and $\Delta t = 0.4$. The obtained results are compared with a reference solution, which is computed considering $\Delta x = 0.1$ and $\Delta t = 0.02$, as well as the standard CD for temporal discretization. The spatial discretization is carried out by the same technique as for the results the respective reference is compared with. In Figures 6–8 results, are presented considering spatial discretizations by the FDM, the FEM with lumped mass matrix and the FEM with consistent mass matrix, respectively. When an iterative procedure is employed, the total amount of iterations is displayed in the plot as well. The results displayed in Figures 6–8 show that in most cases, the proposed stabilized method is more accurate than the other two tested methods. As expected, considering FEM discretizations, better relative performance is obtained by the proposed technique when lumped mass matrices are considered (as it is the case considering the standard CD). For consistent mass matrices, better accuracy may be achieved by the CAAM but with the cost of the solution of several systems of equations within each time step (iterative analysis). The instability of the standard CD for larger time steps is also illustrated in Figures 6–8. As it can be observed, the proposed technique enables the best of two worlds: it ensures stability and eliminates any iterative process when solving complex models. In particular, the accuracy of the results is rather convincing.

5. CONCLUSIONS

In this contribution, a new stabilized central difference approach is introduced, rendering an unconditionally stable time marching technique. As it is illustrated here, the proposed technique is always more accurate than the standard CD and the CAAM, when linear models are considered. In this case, its computational cost is equivalent to that of the CAAM, because one system of equations has to be dealt with at each time step by both procedures. For nonlinear analyses, however, the computational cost of the stabilized CD is considerably lower than that of the CAAM (at least by a factor of two), because no iterative process is required by the new technique. Thus, the proposed methodology provides rather good accuracy and efficiency, being very competitive. Moreover, it is also very easy to implement. In fact, it is just necessary to introduce the AM matrix into a standard CD environment. Finally, different models (linear and nonlinear) have been analyzed, illustrating the good performance of the new technique, even when the standard CD, and the CAAM fail to provide acceptable results.

ACKNOWLEDGEMENTS

The financial supports by *Graduiertenkolleg Seehäfen für Containerschiffe zukünftiger Generationen* (GRK 1096) of the *Deutsche Forschungsgemeinschaft* (DFG), first author, and by CNPq (*Conselho Nacional de Desenvolvimento Científico e Tecnológico*) and FAPEMIG (*Fundação de Amparo à Pesquisa do Estado de Minas Gerais*), second author, are greatly acknowledged.

DOI: 10.1002/nme

REFERENCES

1. Collatz L. *Numerische Behandlung von Differentialgleichungen*, Zweite, neubearbeitete Auflage. Springer-Verlag: Berlin, 1955.
2. Grigorieff RD. *Numerik gewöhnlicher Differentialgleichungen*. Teubner-Verlag: Stuttgart, 1972.
3. Butcher JC. *The Numerical Analysis of Ordinary Differential Equations: Runge–Kutta and General Linear Methods*. Wiley-Interscience: New York, 1987.
4. Wood WL. *Practical Time-Stepping Schemes*, Oxford Applied Mathematics and Computing Science Series. Clarendon Press: Oxford, 1990.
5. Rosenbrock HH. Some general implicit processes for the numerical solution of differential equations. *Computer Journal* 1963; **5**:329–331.
6. Wanner G. On the integration of stiff differential equations. *Numerical Analysis. International Series of Numerical Mathematics* 1977; **37**:209–226. DOI:10.1007/978-3-0348-5575-4_11.
7. Kaps P, Rentrop P. Generalized Runge–Kutta methods of order four with stepsize control for stiff ordinary differential equations. *Numerische Mathematik* 1979; **33**:55–68.
8. Chang SY, Yang YS, Hsu CW. A family of explicit algorithms for general pseudodynamic testing. *Earthquake Engineering and Engineering Vibration* 2011; **10**:51–64. DOI:10.1007/s11803-011-0046-4.
9. Chang SY. Nonlinear evaluations of unconditionally stable explicit algorithms. *Earthquake Engineering and Engineering Vibration* 2009; **8**:329–340. DOI:10.1007/s11803-009-8115-7.
10. Tamma KK, Sha D, Zhou X. Time discretized operators. Part 1: towards the theoretical design of a new generation of a generalized family of unconditionally stable implicit and explicit representations of arbitrary order for computational dynamics. *Computer Methods in Applied Mechanics and Engineering* 2003; **192**:257–290.
11. Sha D, Zhou X, Tamma KK. Time discretized operators. Part 2: towards the theoretical design of a new generation of a generalized family of unconditionally stable implicit and explicit representations of arbitrary order for computational dynamics. *Computer Methods in Applied Mechanics and Engineering* 2003; **192**:291–329.
12. Zhou X, Sha D, Tamma KK. A novel nonlinearly explicit second-order accurate L-stable methodology for finite deformation: hypoelastic/hypoelasto-plastic structural dynamics problems. *International Journal for Numerical Methods in Engineering* 2004; **59**:795–823. DOI:10.1002/nme.878.
13. Soares D. An explicit family of time marching procedures with adaptive dissipation control. *International Journal for Numerical Methods in Engineering* 2014; **100**(3):165–182. DOI:10.1002/nme.4722.
14. Bathe KJ, Wilson EL. Stability and accuracy analysis of direct integration methods. *Earthquake Engineering & Structural Dynamics* 1972; **1**:283–291. DOI:10.1002/eqe.4290010308.
15. Hilber HM, Hughes TJR, Taylor RL. Improved numerical dissipation for time integration algorithms in structural dynamics. *Earthquake Engineering & Structural Dynamics* 1977; **5**:283–292. DOI: 10.1002/eqe.4290050306.
16. Tamma KK, Naburu RR. A robust self-starting explicit computational methodology for structural dynamic applications: Architecture and representations. *International Journal for Numerical Methods in Engineering* 1990; **29**:1441–1454. DOI:10.1002/nme.1620290705.
17. Sha D, Tamma KK, Li M. Robust explicit computational developments and solution strategies for impact problems involving friction. *International Journal for Numerical Methods in Engineering* 1996; **39**:721–739. DOI:10.1002/(SICI)1097-0207(19960315)39:5<721::AID-NME865>3.0.CO;2-J.
18. Soares D. A new family of time marching procedures based on Green's function matrices. *Computers & Structures* 2011; **89**:266–276. DOI:10.1016/j.compstruc.2010.10.011.
19. Soares D. A simple and effective new family of time marching procedures for dynamics. *Computer Methods in Applied Mechanics and Engineering* 2015; **283**:1138–1166. DOI:10.1016/j.cma.2014.08.007.
20. Macek RW, Aubert BH. A mass penalty technique to control the critical time increment in explicit dynamic finite element analyses. *Earthquake Engineering & Structural Dynamics* 1995; **24**:1315–1331. DOI:10.1002/eqe.4290241003.
21. Olovsson L, Unosson M, Simonsson K. Selective mass scaling for thin walled structures modeled with tri-linear solid elements. *Computational Mechanics* 2004; **34**:134–136. DOI: DOI:10.1007/s00466-004-0560-6.
22. Olovsson L, Simonsson K, Unosson M. Selective mass scaling for explicit finite element analyses. *International Journal for Numerical Methods in Engineering* 2005; **63**:1436–1445. DOI:10.1002/nme.1293.
23. Askes H, Nguyen DCD, Tyas A. Increasing the critical time step: micro-inertia, inertia penalties and mass scaling. *Computational Mechanics* 2011; **47**:657–667. DOI:10.1007/s00466-010-0568-z.
24. Cocchetti G, Pagani M, Perego U. Selective mass scaling and critical time-step estimate for explicit dynamic analyses with solid-shell elements. *Computers & Structures* 2013; **127**:39–52. DOI:10.1016/j.compstruc.2012.10.02.
25. Tkachuk A, Bischoff M. Variational methods for selective mass scaling. *Computational Mechanics* 2013; **52**: 563–570. DOI:10.1007/s00466-013-0832-0.
26. Tkachuk A, Bischoff M. Local and global strategies for optimal selective mass scaling. *Computational Mechanics* 2014; **53**:1197–1207. DOI:10.1007/s00466-013-0961-5.
27. Gerschgorin S. Über die Abgrenzung der Eigenwerte einer Matrix. *Bulletin de l'Académie des Sciences de l'URSS. Classe des Sciences Mathématiques et na* 1931; **6**:749–754.